Goldstone models in $D + 1$ dimensions, $D = 3, 4, 5$, supporting stable and zero topological charge solutions



2007 J. Phys. A: Math. Theor. 40 10129

(http://iopscience.iop.org/1751-8121/40/33/013)

IOP Publishing Journal of Physics A: Mathematical and Theoretical

J. Phys. A: Math. Theor. **40** (2007) 10129–10153 doi:10.1088/1751-8113/40/33/013

# Goldstone models in $D + 1$ dimensions, $D = 3, 4, 5$, supporting stable and zero topological charge solutions

**Eugen Radu**[1] **and D H Tchrakian**[1,2]

[1] School of Theoretical Physics—DIAS, 10 Burlington Road, Dublin 4, Ireland
[2] Department of Mathematical Physics, National University of Ireland Maynooth, Ireland

Received 23 May 2007, in final form 4 July 2007
Published 1 August 2007
Online at stacks.iop.org/JPhysA/40/10129

**Abstract**

We study finite energy static solutions to a global symmetry breaking Goldstone model described by an isovector scalar field in $D + 1$ spacetime dimensions. Both topologically stable multisolitons with arbitrary winding numbers and zero topological charge soliton–antisoliton solutions are constructed numerically in $D = 3, 4, 5$. We have explored the types of symmetries the systems should be subjected to, for there to exist multisoliton and soliton–antisoliton pairs in $D = 3, 4, 5, 6$. These findings are underpinned by constructing numerical solutions in the $D \leqslant 5$ examples. Subject to axial symmetry, only multisolitons of all topological charges exist in *even* $D$, and in *odd* $D$ only zero and unit topological charge solutions exist. Subjecting the system to weaker than axial symmetries results in the existence of all the possibilities in all dimensions. Our findings also apply to finite 'energy' solutions to Yang–Mills and Yang–Mills–Higgs systems as well as to sigma models, but we find the numerical work for the Goldstone models more accessible.

PACS numbers: 11.10.−z, 12.10.−g, 12.15.−y

## 1. Introduction

Very early in the history of field theory solitons interest in the existence of zero topological charge solutions arose. In the case of the Yang–Mills (YM) instantons [1] in $D = 4$ Euclidean space, which are self-dual, this raised the question of the existence of non-self-dual [2–4] solutions, while even earlier this question was investigated [5] in the case of magnetic monopoles of the YM–Higgs (YMH) model in $D = 3$ [6]. More recently, concrete numerical constructions of monopole–antimonopole solutions [7–9] to the YMH model in $D = 3$, instanton–antiinstanton solutions [10] to the YM model in $D = 4$, as well as soliton–antisoliton solutions [11] to a Goldstone model in $D = 3$, were given.

The potential relevance of field theory soliton–antisolitons in higher dimensions rests in the fact that they describe non-BPS field configurations that may be useful in the description of brane–antibrane configurations. Non-BPS configurations are relevant for example in the context of string junctions in $N = 4$ super-Yang–Mills [12]. Such solutions can be the zero topological charge counterparts of higher dimensional instantons [13] and of monopoles [14] or of the solitons of the symmetry breaking Goldstone-type models [15] arising as the gauge decoupling limits of higher dimensional monopole models [14]. These Goldstone models have not found any physical applications to date, but as prototype systems modelling higher dimensional monopoles without the burden of gauge degrees of freedom they can be useful for example in providing backgrounds on which Dirac equations [16] in all dimensions can be solved or possibly also for gravitating monopoles. Here, they will prove very useful in studying zero topological charge solutions in higher dimensions.

Zero topological charge solutions to such a Goldstone model in $D = 3$ were recently given in [11]. The model in [11] is the gauge decoupling limit of the YMH model descending from the $p = 2$ member of the YM hierarchy introduced in [13] and is the simplest example. In the present paper, we will extend this study to the Goldstone model descending from the $p = 3$ member of the YM hierarchy. In contrast to the $p = 2$ Goldstone model which supports finite energy solitons only in $D = 3$, the $p = 3$ Goldstone model enables us to study solutions in dimensions $D = 3, 4, 5$, allowed by the Derrick scaling rule. This is very important for our purposes here as will be explained below. As such, the $p = 3$ Goldstone model will serve as a vehicle for us to investigate zero topological charge solutions in the simplest possible technical setting.

The main objective of this work is to find out subject to what symmetries and for what boundary conditions do such solutions exist? We have presented several numerically constructed solutions in dimensions $D \leqslant 5$, by way of underpinning our findings. While our symmetry considerations cover the dimensions $3 \leqslant D \leqslant 6$, the concrete numerical constructions are limited to $D = 3, 4, 5$ in the $p = 3$ Goldstone model, covering both even and odd dimensions, allowing us to make a classification of the said conditions. Our study addresses the question as to what are the requisite ingredients in the construction of zero topological charge solitons in higher dimensions, highlighting the distinction between even and odd dimensions in this respect. We find that such solutions can be accommodated by imposing the requisite boundary conditions for systems subject to the appropriate symmetry, in all dimensions. Stated most succinctly, subject to axial symmetry only multisolitons of arbitrary charges exist in even $D$, while in odd $D$ zero and unit topological charge solutions can exist. By imposing less stringent symmetries than axial, all possible types of solutions can be constructed in any dimension.

The symmetries considered are at one extreme *axial*, namely spherical symmetry in an $\mathbb{R}^{D-1}$ subspace of $\mathbb{R}^D$, and at the other *azimuthal*, namely rotational symmetry in an $\mathbb{R}^2$ subspace of $\mathbb{R}^D$. In between, we have explored the imposition of all *intermediate* cases, namely the imposition of rotational symmetry in all the other subspaces $\mathbb{R}^n$ of $\mathbb{R}^D$. In addition, we have considered the imposition of multi-azimuthal symmetries on all $\mathbb{R}^2$ subspaces of $\mathbb{R}^D$.

Concerning the numerical constructions, our reason for limiting to the $p = 3$ Goldstone model, and to $D \leqslant 5$, is that otherwise it would be necessary to carry out numerical integrations in more than two dimensions, which is beyond the scope of this work.

In section 2, we have introduced the models to be employed, along with the topological charge densities providing the lower bounds on the energies. Section 3 is concerned with the imposition of symmetries, i.e. stating the axial, azimuthal, intermediate and multi-azimuthal Ansätze. In particular, the energy density functionals of the model, for the dimensions in which numerical solutions will be constructed, are subjected to the spherical, axial and bi-azimuthal

symmetries. Subjecting the corresponding topological charge densities to symmetries is carried out in section 4. Section 5 contains all the numerical results, which verify the assertions presented in the previous section, section 4, concerning the symmetry properties that zero topological charge solutions must have. In section 6, we summarize our results and extend the discussion of symmetries to beyond the particular simple models employed here.

## 2. The model and the topological charge

The symmetry breaking models in $D=3,4$ and 5 spatial dimensions, to which we refer as the Goldstone models, are described by a scalar isovector field $\phi^a$, $a=1,2,3$, $a=1,2,3,4$ and $a=1,2,3,4,5$, in each dimension, respectively.

There is such a hierarchy of models [15] that arise from the gauge-decoupled limit of the $D$-dimensional $SO(D)$ gauged Higgs (YMH) model descended from the $p$th member of the Yang–Mills (YM) hierarchy on $\mathbb{R}_D \times S^{4p-D}$. Here, we have chosen the simplest of these that can accommodate $D=3,4,5$, while satisfying the Derrick scaling requirement for the existence of finite energy solutions. In the present case, this is the YMH model that descends from the $p=3$ rd member of the YM hierarchy. Our Goldstone model here is the gauge-decoupled limit of this YMH system. Using the notation

$$\phi^a_\mu = \partial_\phi \mu^a, \qquad \phi^{ab}_{\mu\nu} = \partial_{[\mu}\phi^a\partial_{\nu]}\phi^b, \qquad \phi^{abc}_{\mu\nu\rho} = \partial_{[\mu}\phi^a\partial_\nu\phi^b\partial_{\rho]}\phi^c,$$

with the brackets $[\mu\nu\cdots]$ implying total antisymmetrization, the static energy density is

$$\mathcal{E}_{(p=3)} = \lambda_0(\eta^2-|\phi^a|^2)^6 + \lambda_1(\eta^2-|\phi^b|^2)^4\left|\phi^a_\mu\right|^2 + \lambda_2(\eta^2-|\phi^b|^2)^2\left|\phi^{ab}_{\mu\nu}\right|^2 + \lambda_3\left|\phi^{abc}_{\mu\nu\rho}\right|^2. \quad (1)$$

All the dimensionless constants $\lambda_0$, $\lambda_1$, $\lambda_2$ and $\lambda_3$ must be positive if the relevant topological lower bounds in each dimension are to be valid. The model (1) is ad hoc rather than a dimensionally descended, only insofar as the numerical values of these dimensionless coupling constants, which are otherwise fixed by the descent mechanism, are constrained only to be positive. Of course, any of these constants can also vanish, provided that the absence of the corresponding term in (1) does not violate the Derrick scaling requirement.

The most important feature of the models such as (1) is that the order parameter field $\phi^a$ is a relic of a Higgs field and has the same dimensions ($L^{-1}$) as a connection, and the finite energy conditions allow the symmetry breaking boundary conditions

$$\lim_{R\to 0}|\phi^a| = 0, \qquad \lim_{R\to\infty}|\phi^a| = \eta, \quad (2)$$

with $R$ being the radial coordinate in $\mathbb{R}^D$, this resulting in *monopole*-like asymptotics for our solitons.

The presence of the symmetry breaking potential in (1), multiplying $\lambda_0$, has no quantitative effect on the solutions, so it will be ignored henceforth.

In the next section, where symmetries will be imposed, we will concentrate only on the terms

$$\left|\phi^a_\mu\right|^2, \qquad \left|\phi^{ab}_{\mu\nu}\right|^2, \qquad \left|\phi^{abc}_{\mu\nu\rho}\right|^2 \quad (3)$$

and will delay the incorporation of the factors $(\eta^2-|\phi^b|^2)^2$ and $(\eta^2-|\phi^b|^2)^4$ till the section on numerics, since the imposition of symmetries on these last terms is achieved rather trivially.

The topological charge density bounding the energy density functional from below can be stated simply in terms of Bogomol'nyi inequalities, separately for each dimension $D=3,4$ and 5.

In $D=3$, the inequality

$$(\eta^2-|\phi|^2)^2\left|(\eta^2-|\phi|^2)\phi^c_\rho - \frac{1}{2!^2}\varepsilon_{\mu\nu\rho}\varepsilon^{abc}\phi^{ab}_{\mu\nu}\right|^2 \geqslant 0 \quad (4)$$

leads to the lower bound[3]

$$(\eta^2-|\phi|^2)^4\left|\phi^a_\mu\right|^2+\tfrac{1}{4}(\eta^2-|\phi|^2)^2\left|\phi^{ab}_{\mu\nu}\right|^2\geqslant\varepsilon_{\mu\nu\rho}\varepsilon^{abc}(\eta^2-|\phi|^2)^3\phi^a_\mu\phi^b_\nu\phi^c_\rho\equiv\varrho_3. \tag{5}$$

In (4) and (5), we have denoted $|\phi^a|^2$ by $|\phi|^2$.

In $D=4$, the inequalities

$$\begin{aligned}&(\eta^2-|\phi|^2)^2\left|\phi^{ab}_{\mu\nu}-\frac{1}{2!^2}\varepsilon_{\mu\nu\rho\sigma}\varepsilon^{abcd}\phi^{cd}_{\rho\sigma}\right|^2\geqslant 0\\&\left|(\eta^2-|\phi|^2)^2\phi^c_\rho-\frac{1}{3!}\varepsilon_{\mu\nu\rho\sigma}\varepsilon^{abcd}\phi^{abc}_{\mu\nu\rho}\right|^2\geqslant 0\end{aligned} \tag{6}$$

lead to the lower bound

$$\begin{aligned}&\tfrac{1}{4}(\eta^2-|\phi|^2)^4\left|\phi^a_\mu\right|^2+\tfrac{1}{2}(\eta^2-|\phi|^2)^2\left|\phi^{ab}_{\mu\nu}\right|^2+\tfrac{1}{4}\left|\phi^{abc}_{\mu\nu\rho}\right|^2\\&\qquad\geqslant\varepsilon_{\mu\nu\rho\sigma}\varepsilon^{abcd}(\eta^2-|\phi|^2)^2\phi^a_\mu\phi^b_\nu\phi^c_\rho\phi^d_\sigma\equiv\varrho_4.\end{aligned} \tag{7}$$

In $D=5$, the inequality

$$\left|(\eta^2-|\phi|^2)\phi^{ab}_{\mu\nu}-\tfrac{1}{2^2 3!}\varepsilon_{\mu\nu\rho\sigma\tau}\varepsilon^{abcde}\phi^{cde}_{\rho\sigma\tau}\right|^2\geqslant 0$$

leads to the lower bound

$$(\eta^2-|\phi|^2)^2|\phi^{ab}_{\mu\nu}|^2+\tfrac{1}{4}\left|\phi^{abc}_{\mu\nu\rho}\right|^2\geqslant\varepsilon_{\mu\nu\rho\sigma\tau}\varepsilon^{abcde}(\eta^2-|\phi|^2)\phi^a_\mu\phi^b_\nu\phi^c_\rho\phi^d_\sigma\phi^e_\tau\equiv\varrho_5. \tag{8}$$

Each of the three topological charge densities $\varrho_3$, $\varrho_4$ and $\varrho_5$ is a total divergence, which we denote as $\varrho_3=\partial_\mu\Omega^{(3)}_\mu$, $\varrho_4=\partial_\mu\Omega^{(4)}_\mu$ and $\varrho_5=\partial_\mu\Omega^{(5)}_\mu$, respectively; the surface integrals of $\Omega^{(D)}_\mu$ yielding the topological charge in each dimension $D=3,4,5$. In this paper, we will refer to the densities $\Omega^{(D)}_\mu$ as *topological currents*. Now these topological charge densities are simply numerical multiples of the respective winding number densities

$$\varrho^{(0)}_D=\varepsilon_{\mu_1\mu_1\ldots\mu_D}\varepsilon^{a_1a_2\ldots a_D}\phi^{a_1}_{\mu_1}\phi^{a_2}_{\mu_2}\cdots\phi^{a_D}_{\mu_D}\equiv\partial_{\mu_1}\omega^{(D)}_{\mu_1} \tag{9}$$

which are the surface integrals of the winding number *currents*

$$\omega^{(D)}_{\mu_1}=\varepsilon_{\mu_1\mu_1\ldots\mu_D}\varepsilon^{a_1a_2\ldots a_D}\phi^{a_1}\phi^{a_2}_{\mu_2}\cdots\phi^{a_D}_{\mu_D}. \tag{10}$$

The topological charges $q_3$, $q_4$ and $q_5$, which are the volume integrals of the densities $\varrho_3$, $\varrho_4$ and $\varrho_5$ defined in (5), (7) and (8) respectively, are in turn equal to the surface integrals of the topological currents

$$\begin{aligned}\Omega^{(3)}_\mu&=\varepsilon_{\mu\nu\rho}\varepsilon^{abc}\left[\eta^6-\tfrac{9}{5}\eta^4|\phi|^2+\tfrac{9}{7}\eta^2(|\phi|^2)^2-\tfrac{1}{3}(|\phi|^2)^3\right]\phi^a\phi^b_\nu\phi^c_\rho\\\Omega^{(4)}_\mu&=\varepsilon_{\mu\nu\rho\sigma}\varepsilon^{abcd}\left[\eta^4-\tfrac{4}{3}\eta^2|\phi|^2+\tfrac{1}{2}\eta^2(|\phi|^2)^2\right]\phi^a\phi^b_\nu\phi^c_\rho\phi^d_\sigma\\\Omega^{(5)}_\mu&=\varepsilon_{\mu\nu\rho\sigma\tau}\varepsilon^{abcde}\left[\eta^2-\tfrac{5}{7}\eta^2|\phi|^2\right]\phi^a\phi^b_\nu\phi^c_\rho\phi^d_\sigma\phi^e_\tau.\end{aligned} \tag{11}$$

It is now obvious, in light of the asymptotic boundary value in (2), that $q_3$, $q_4$ and $q_5$ are the multiples of the winding numbers, namely the surface integrals of the currents (10), with the numbers $\frac{16}{105}$, $\frac{1}{6}$ and $\frac{1}{7}$, respectively.

[3] Note that the $D=3$ model employed here is slightly different from that in [11], the latter being the gauge-decoupled version of the $p=2$ YMH model, in contrast to the gauge-decoupled version of the $p=3$ YMH model here.

## 3. Imposition of symmetries

This section is divided into four subsections, in each of which the three building blocks in (3) will be subjected to spherical, axial, azimuthal, and in four dimensions only, and the bi-azimuthal symmetries, respectively. We shall also state the tri-azimuthal Ansatz, only in six dimensions, but will not display the building blocks (3) subject to it because in six dimensions the Derrick scaling requires an *octic* term beyond these, whose numerical pursuit is beyond the scope of this work. The symmetry breaking self-interaction potential $(\eta^2-|\phi^a|^2)^6$ will be ignored, instead the boundary condition (2) it would enforce will be imposed directly.

Imposition of symmetry is the first step in the construction of zero topological charge solutions, leading to the second step of selecting the requisite boundary conditions to achieve this aim. In this section, we impose the symmetries on the energy density functional (1) whose second-order equations will be integrated numerically in section 5, deferring the task of imposing symmetries on the topological charge densities (9) and their currents (10) to the next section, section 4. There, the most important task of selecting the requisite boundary conditions will be made.

Before stating the Ansätze pertaining to the various symmetries to be imposed on the scalar field $\phi^a$ describing the model (1), we introduce the coordinates to be employed in each case. Next to spherical symmetry, the strongest symmetry that we will impose is the *axial* symmetry, sometimes also described as *cylindric* symmetry. This involves the imposition of rotational symmetry in an $\mathbb{R}^{D-1}$ subspace of the full space $\mathbb{R}^D$. The weakest symmetry is the *azimuthal* one, which involves the imposition of rotational symmetry in an $\mathbb{R}^2$ subspace of $\mathbb{R}^D$. Then, there are all the *intermediate* symmetries involving the imposition of rotational symmetry in an $\mathbb{R}^n$ subspace of $\mathbb{R}^D$, with $D-2\geqslant n\geqslant 3$. As we restrict to $D=5$, the only relevant values of $n$ are $n=3$ and 4. In addition, we will employ *multi-azimuthal* symmetries, each one of its constituent azimuthal symmetries being imposed on distinct planes in $\mathbb{R}^D$. Since we will restrict to $D=6$, our attention will be restricted to the *bi-azimuthal* and *tri-azimuthal* cases only. The coordinates are parametrized as follows.

*Axial coordinates.* In this case, we label the coordinate on $\mathbb{R}^D$ as follows:

$$x_\mu=(x_i,x_D),\qquad i=1,2,\ldots,D-1,\qquad |x_i|^2=r^2,\qquad R^2=r^2+x_D^2, \tag{12}$$

so that

$$r=R\sin\theta_1,\qquad x_D=R\cos\theta_1, \tag{13}$$

where $\theta_1$ is the leading polar angle in each dimension, parametrized by the spherical polar angles $(\theta_1,\theta_2,\ldots,\theta_{D-3},\theta_{D-2},\varphi)$, with $\varphi$ being the azimuthal angle (with $0\leqslant\varphi\leqslant 2\pi$, $0\leqslant\theta_i\leqslant\pi$). Our definition of axial symmetry amounts to spherical symmetry in the $(D-1)$-dimensional subspace, as for example in [17].

*Azimuthal coordinates.* Imposing azimuthal symmetry in the $x_i=(x_1,x_2)$ plane leaves the dependence of the fields on the coordinates $x_I=(x_3,x_4,\ldots,x_D)$ unrestricted. In practice, however, we will restrict to the $D=4$ case only for reasons explained in section 4. The labelling we will employ is

$$x_\mu=(x_i,x_I),\qquad i=1,2,\qquad I=3,4,\qquad |x_i|^2=\rho^2,\qquad R^2=\rho^2+|x_I|^2, \tag{14}$$

so that

$$\rho=R\sin\theta_1\sin\theta_2,\qquad x_3=R\sin\theta_1\cos\theta_2,\qquad x_4=R\cos\theta_1, \tag{15}$$

or

$$\rho=r\sin\theta_2,\qquad x_3=z=r\cos\theta_2,\qquad x_4=t. \tag{16}$$

*Intermediate coordinates.* In $D = 5$, the only *intermediate* possibility is $n = 3$, and we label the coordinate as

$$x_\mu = (x_i, x_4, x_5) \equiv (x_i, s, t), \qquad i = 1, 2, 3, \qquad |x_i|^2 = r^2, \qquad R^2 = r^2 + s^2 + t^2, \tag{17}$$

so that

$$r = R \sin\theta_1 \sin\theta_2, \qquad s = R \sin\theta_1 \cos\theta_2, \qquad t = R \cos\theta_1, \tag{18}$$

in an angular parametrization $(\theta_1, \theta_2, \theta_3, \varphi)$, with polar angles ranging from 0 to $\pi$, with $\varphi$ being the azimuthal angle ranging from 0 to $2\pi$. The notation

$$\hat{x}_i = (\sin\theta_3 \cos\varphi, \sin\theta_3 \sin\varphi, \cos\theta_3) \tag{19}$$

will be employed below.

In $D = 6$, both $n = 3$ and $n = 4$ are possible, but the second leads to a four-dimensional effective system which is superfluous for our purposes here. Hence, we restrict to $n = 3$ and label the coordinate as

$$x_\mu = (x_i, x_5, x_6) \equiv (x_i, s, t), \qquad i = 1, 2, 3, 4, \qquad |x_i|^2 = r^2, \qquad R^2 = r^2 + s^2 + t^2, \tag{20}$$

so that $(r, s, t)$ are parametrized exactly as in (18) in an angular parametrization $(\theta_1, \theta_2, \theta_3, \theta_4, \varphi)$. The notation

$$\hat{x}_i = (\sin\theta_3 \sin\theta_4 \cos\varphi, \sin\theta_3 \sin\theta_4 \sin\varphi, \sin\theta_3 \cos\theta_4, \cos\theta_3) \tag{21}$$

being employed for this case below.

*Bi-azimuthal coordinates.* In this case, we will restrict our attention to $D = 4$ and $D = 5$. (Bi-azimuthal symmetry in $D = 6$ would lead to four-dimensional residual subsystems, which are superfluous for our purposes here.) In the first case, we will subject the components of the energy density functional (3) to the symmetry implied by the Ansatz, while in the second case, we will only state the Ansatz since no solutions will be constructed subsequently in that case.

In $D = 4$, we impose a second azimuthal symmetry in (14), in the $x_I = (x_3, x_4)$ plane, denoting the radial variable in the $(x, y)$ and $(z, t)$ planes with $\rho = \sqrt{x^2 + y^2} = \sqrt{|x_i|^2}$ and $\sigma = \sqrt{z^2 + t^2} = \sqrt{|x_I|^2}$. In this case, we will parametrize $\mathbb{R}^4$ as

$$\begin{aligned} x_i &= (R \sin\psi)\hat{x}_i \equiv \rho\hat{x}_i, \qquad \hat{x}_i = (\cos\varphi_1, \sin\varphi_1) \\ x_I &= (R \cos\psi)\hat{x}_I \equiv \sigma\hat{x}_I, \qquad \hat{x}_I = (\cos\varphi_2, \sin\varphi_2) \end{aligned} \tag{22}$$

where $R^2 = |x_i|^2 + |x_I|^2 = |x_\mu|^2$, with $0 \leqslant \psi \leqslant \frac{\pi}{2}$, $0 \leqslant \varphi_1 \leqslant 2\pi$ and $0 \leqslant \varphi_2 \leqslant 2\pi$. While the two angles $(\varphi_1, \varphi_2)$ are azimuthal angles, the angle $\theta$ here is not a polar angle as its range is one-half of that of a polar angle. We shall refer to such angles as semi-polar henceforth.

In $D = 5$, $\mathbb{R}^5$ is parametrized as

$$x_i = (R \sin\theta \sin\psi)\hat{x}_i \equiv r\hat{x}_i, \qquad \hat{x}_i = (\cos\varphi_1, \sin\varphi_1) \tag{23}$$

$$x_I = (R \sin\theta \cos\psi)\hat{x}_I \equiv s\hat{x}_I, \qquad \hat{x}_I = (\cos\varphi_2, \sin\varphi_2) \qquad x_5 = R\cos\theta \equiv t \tag{24}$$

where $R^2 = r^2 + s^2 + t^2$, and $0 \leqslant \theta \leqslant \pi$ and $0 \leqslant \psi \leqslant \frac{\pi}{2}$. In (23) and (25), $\theta$ is a polar angle and $\psi$ a semi-polar angle. We denote polar angles by $\theta$ and semi-polar angles by $\psi$ henceforth. All azimuthal angles are likewise denoted by $\varphi$.

*Tri-azimuthal coordinates.* Here, we restrict our attention to $D = 6$ only for reasons explained already. Extending the labelling (22) of $\mathbb{R}^4$ to that of $\mathbb{R}^6$, with $\rho = \sqrt{x_1^2 + x_2^2} =$

$\sqrt{|x_{i_1}|^2}, i_1 = 1,2, \sigma = \sqrt{x_3^2+x_4^2} = \sqrt{|x_{i_2}|^2}, i_2 = 3,4$ and $\tau = \sqrt{x_5^2+x_6^2} = \sqrt{|x_{i_3}|^2}, i_3 = 5,6$, by

$$\begin{aligned} x_{i_1} &= (R\sin\psi_1\sin\psi_2)\hat{x}_{i_1} \equiv \rho\hat{x}_{i_1}, & \hat{x}_{i_1} &= (\cos\varphi_1, \sin\varphi_1) \\ x_{i_2} &= (R\sin\psi_1\cos\psi_2)\hat{x}_{i_2} \equiv \sigma\hat{x}_{i_2}, & \hat{x}_{i_2} &= (\cos\varphi_2, \sin\varphi_2) \\ x_{i_3} &= (R\cos\psi_1)\hat{x}_{i_3} \equiv \tau\hat{x}_{i_3}, & \hat{x}_{i_3} &= (\cos\varphi_3, \sin\varphi_3) \end{aligned} \tag{25}$$

where $R^2 = |x_{i_1}|^2 + |x_{i_2}|^2 + |x_{i_3}|^2 = |x_\mu|^2$, with $0 \leqslant \psi_1 \leqslant \frac{\pi}{2}$, $0 \leqslant \psi_2 \leqslant \frac{\pi}{2}$, and with the three azimuthal angles $0 \leqslant \varphi_1 \leqslant 2\pi$, $0 \leqslant \varphi_2 \leqslant 2\pi$ and $0 \leqslant \varphi_3 \leqslant 2\pi$.

### *3.1. Spherical symmetry*

The spherically symmetric Ansatz for the scalar field $\phi^a$ in $D$ dimensions is

$$\phi^a = \eta Q(R)\hat{x}^a, \qquad \hat{x}^a = \frac{x^a}{R}, \tag{26}$$

resulting in the reduced building blocks (3)

$$\begin{aligned} \left|\phi^a_\mu\right|^2 &= Q_R^2 + (D-1)\left(\frac{Q}{R}\right)^2 \\ \left|\phi^{ab}_{\mu\nu}\right|^2 &= 2(D-1)\left(\frac{Q}{R}\right)^2\left[2Q_R^2 + (D-2)\left(\frac{Q}{R}\right)^2\right] \\ \left|\phi^{abc}_{\mu\nu\rho}\right|^2 &= 6(D-1)(D-2)\left(\frac{Q}{R}\right)^4\left[3Q_R^2 + (D-3)\left(\frac{Q}{R}\right)^2\right] \end{aligned} \tag{27}$$

where we have used the notation $Q_R = \frac{\partial Q}{\partial R}$ .

### *3.2. Axial symmetry*

The axially symmetric Ansatz for the scalar field $\phi^a = (\phi^\alpha, \phi^D)$ in $D \geqslant 4$ dimensions, with the index $\alpha = 1, 2, \ldots, D-1$ is

$$\phi^\alpha = \eta H(r, x_D)\hat{x}^\alpha, \qquad \phi^D = \eta G(r, x_D), \qquad \hat{x}^\alpha = \frac{x^\alpha}{r}, \tag{28}$$

using the labelling (12) of the coordinates.

There is a very important exception in the $D=3$ case of (28), where the imposition of axial symmetry on the field $\phi^a = (\phi^A, \phi^3)$, $A = 1,2$, is tantamount to imposing azimuthal symmetry. The axially symmetric Ansatz in $D=3$ is

$$\phi^A = \eta H(r, x_3)n^A, \qquad \phi^3 = \eta G(r, x_3), \qquad n^A = \begin{bmatrix}\cos n\varphi \\ \sin n\varphi\end{bmatrix}, \tag{29}$$

with $n = 1, 2, 3, \ldots$ being the azimuthal vortex number.

The result of substituting (28) into (3) is

$$\left|\phi^a_\mu\right|^2 = \left(H_r^2 + G_r^2 + H_D^2 + G_D^2\right) + (D-2)\left(\frac{H}{r}\right)^2,$$

$$\frac{1}{2}\left|\phi^{ab}_{\mu\nu}\right|^2 = 2(H_{[r}G_{D]})^2 + (D-2)\left(\frac{H}{r}\right)^2\left[2\left(H_r^2 + G_r^2 + H_D^2 + G_D^2\right) + (D-3)\left(\frac{H}{r}\right)^2\right],$$

$$\frac{1}{6}\left|\phi^{abc}_{\mu\nu\rho}\right|^2 = (D-2)\left(\frac{H}{r}\right)^2\left\{6(H_{[r}G_{D]})^2 + (D-3)\left(\frac{H}{r}\right)^2\left[3\left(H_r^2+G_r^2+H_D^2+G_D^2\right)+(D-4)\left(\frac{H}{r}\right)^2\right]\right\}, \tag{30}$$

where we have used the notation $H_r = \frac{\partial H}{\partial r}$, $H_D = \frac{\partial H}{\partial x_D}$ and $H_{[r}G_{D]} = (H_rG_D - H_DG_r)$.

The spherically symmetric limit (27) of (30) follows immediately from (13), by the replacements

$$H(r,x_D) = Q(R)\sin\theta_{D-2}, \qquad G(r,x_D) = Q(R)\cos\theta_{D-2},$$

with $R^2 = r^2 + x_D^2$, and using

$$\partial_r = \sin\theta_{D-2}\partial_R + \frac{\cos\theta_{D-2}}{R}\partial_{\theta_{D-2}}, \qquad \partial_D = \cos\theta_{D-2}\partial_R - \frac{\sin\theta_{D-2}}{R}\partial_{\theta_{D-2}}.$$

### *3.3. Azimuthal symmetry*

This subsection is concerned with the imposition of azimuthal symmetry in a $D$-dimensional system, resulting in a $(D-1)$-dimensional residual subsystem. As such, it does not lead to a boundary-value problem which can be tackled numerically in a practical way. It should thus be viewed as a first step towards the imposition of bi-azimuthal symmetry in the $D = 2+2 = 4$ case presented in the next subsection.

Imposing azimuthal symmetry in the $x_i = (x_1, x_2)$ subspace (plane) of $x_\mu = (x_i, x_I)$, $I = 3, 4, \ldots, D$, and labelling the scalar field as $\phi^a = (\phi^A, \phi^{A'})$, $A = 1, 2$ and $A' = 3, 4, \ldots, D$, the components $\phi^A$ are restricted by the Ansatz

$$\phi^A = h(\rho, x_I)n^A, \qquad n^A = (\cos n\varphi, \sin n\varphi), \qquad \rho^2 = |x_i|^2 = x^2 + y^2, \tag{31}$$

while the $D-2$ components $\phi^{A'} = \phi^{A'}(\rho, x_I)$ retain their dependence on the $D-2$ coordinates $x_I$.

The result of enforcing the Ansatz (31) is most compactly expressed by employing the coordinate $x_M = (x_I, \rho)$, and by labelling the residual field as $\chi^\alpha = (\chi^{A'}, \chi^{D-1}) \equiv (\phi^{A'}, h)$, with the new index running over $\alpha = A', D-1$. In this notation, we have

$$\begin{aligned}
\left|\phi^a_\mu\right|^2 &= \left(\frac{n\chi^{D-1}}{\rho}\right)^2 + |\partial_M\chi^\alpha|^2 \\
\frac{1}{2}\left|\phi^{ab}_{\mu\nu}\right|^2 &= 4\left(\frac{n\chi^{D-1}}{\rho}\right)^2|\partial_M\chi^\alpha|^2 + |\partial_{[M}\chi^\alpha\partial_{N]}\chi^\beta|^2 \\
\frac{1}{6}\left|\phi^{abc}_{\mu\nu\rho}\right|^2 &= \frac{5}{2}\left(\frac{n\chi^{D-1}}{\rho}\right)^2|\partial_M\chi^\alpha|^2 + |\partial_{[M}\chi^\alpha\partial_{N]}\chi^\beta|^2 + \frac{1}{6}|\partial_{[M}\chi^\alpha\partial_N\chi^\beta\partial_{R]}\chi^\gamma|^2.
\end{aligned} \tag{32}$$

In the case of interest here, namely for $D = 4$, $x_\mu = (x_i, x_I)$, with $i = 1, 2 = x, y$ and $I = 3, 4 = z, t$, the azimuthally symmetric Ansatz (31) now becomes

$$\phi^A = h(\rho, z, t)n^A, \qquad \phi^{A'} = \chi^{A'}(x_I, \rho) = \begin{bmatrix} f(\rho, z, t) \\ g(\rho, z, t) \end{bmatrix}, \tag{33}$$

resulting in the residual three-dimensional system with coordinates $x_M = (z, t, \rho)$ being given by (32) with $\chi^{D-1} = \chi^3 \equiv h$.

The axially symmetric limit (30) of (32) follows immediately from (15), by the replacements

$$h(z,t,\rho) = H(r,t)\sin\theta_1 \quad , \qquad f(z,t,\rho) = H(r,t)\cos\theta_1 \quad , \quad g(z,t,\rho) = G(r,t),$$

with $r^2=\rho^2+z^2$, and using

$$\partial_\rho = \sin\theta_1\partial_r + \frac{\cos\theta_1}{r}\partial_{\theta_1}, \qquad \partial_z = \cos\theta_1\partial_r - \frac{\sin\theta_1}{r}\partial_{\theta_1}.$$

### *3.4. Intermediate symmetries*

The symmetries to be considered here are rotational symmetry in the $\mathbb{R}^3$ subspace of $\mathbb{R}^5$ (for $D=5$) and the $\mathbb{R}^4$ subspace of $\mathbb{R}^6$ (for $D=6$). (Rotational symmetry in the $\mathbb{R}^3$ subspace of $\mathbb{R}^6$ would be superfluous since that would lead to a four-dimensional effective system.)

For $D=5$, the intermediate symmetric Ansatz for the field $\phi^a=(\phi^\alpha,\phi^4,\phi^5)$ is

$$\phi^\alpha = \eta h(r,s,t)\hat{x}^\alpha, \qquad \phi^4=\eta g(r,s,t), \qquad \phi^5=\eta f(r,s,t) \tag{34}$$

using the notation of (17)–(19).

The intermediate symmetric Ansatz for the field $\phi^a=(\phi^\alpha,\phi^5,\phi^6)$ for $D=6$ is

$$\phi^\alpha = \eta h(r,s,t)\hat{x}^\alpha, \qquad \phi^5=\eta g(r,s,t), \qquad \phi^6=\eta f(r,s,t) \tag{35}$$

which looks formally identical to (34), but now the coordinates being read from (20) and (21).

In both cases, the system reduces to a three-dimensional effective subsystems, for which numerical constructions are outside the scope of this work. Hence, we do not display the result of symmetry imposition on the energy density functionals (3).

### *3.5. Bi-azimuthal symmetry*

Our considerations in this subsection cover two cases, namely to state the bi-azimuthal Ansätze in $D=4$ and $D=5$. The residual subsystem in each case is two dimensional and three dimensional, respectively. In the first case we will construct the solutions numerically, so the Ansatz will be imposed on the energy density functional, while in the second we will limit ourselves to stating the Ansatz.

*Bi-azimuthal symmetry in $D=4$.* In the $D=4$ case, using the notation (22) for the coordinates and using the same notation (31) as in subsection 3.3, $\phi^a=(\phi^A,\phi^{A'})$, the bi-azimuthally symmetric Ansatz is

$$\begin{aligned} \phi^A &= \eta h(\rho,\sigma)n_1^A, & n_1^A &= (\cos n_1\varphi_1, \sin n_1\varphi_1),\\ \phi^{A'} &= \eta g(\rho,\sigma)n_2^{A'}, & n_2^{A'} &= (\cos n_2\varphi_2, \sin n_2\varphi_2), \end{aligned} \tag{36}$$

where $n_1$ and $n_2$ are the respective vorticities in the two planes.

In fact, the Ansatz (36) results in the first stage from the imposition of azimuthal symmetry (31) in $D=4$, with the residual fields $\chi^\alpha=(\phi^{A'},h)$, and then imposing a second stage of azimuthal symmetry on the triplet $\chi^\alpha$. Concerning the imposition of the second stage of azimuthal symmetry, we point out that the densities (32) resulting from the first stage do not exhibit a global $SO(D-1)$ invariance, although the original densities (3) are invariant under a global $SO(D)$.[4] We have verified that the second stage results a consistent reduction, even though the reduced system after the first stage did not possess a global invariance.

Imposition of bi-azimuthal symmetry enables a two-dimensional boundary-value problem, to be tackled numerically in the next section, so we list the resulting densities (3)

[4] This is in contrast to that of a YM system, where the local gauge group does, under azimuthal symmetry imposition, reduce to an effective YM–Higgs system exhibiting a broken local gauge invariance [10].

$$
\begin{aligned}
\left|\phi^a_\mu\right|^2 &= \left[\left(\frac{n_1 h}{\rho}\right)^2 + \left(\frac{n_2 g}{\sigma}\right)^2\right] + \left(h_\rho^2 + g_\rho^2 + h_\sigma^2 + g_\sigma^2\right), \\
\frac{1}{2!^2}\left|\phi^{ab}_{\mu\nu}\right|^2 &= \left(\frac{n_1 h}{\rho}\right)^2\left(\frac{n_2 g}{\sigma}\right)^2 + \left[\left(\frac{n_1 h}{\rho}\right)^2 + \left(\frac{n_2 g}{\sigma}\right)^2\right]\left(h_\rho^2 + g_\rho^2 + h_\sigma^2 + g_\sigma^2\right) + (h_{[\rho}g_{\sigma]})^2, \\
\frac{1}{3!^2}\left|\phi^{abc}_{\mu\nu\rho}\right|^2 &= \left(\frac{n_1 h}{\rho}\right)^2\left(\frac{n_2 g}{\sigma}\right)^2\left(h_\rho^2 + g_\rho^2 + h_\sigma^2 + g_\sigma^2\right) + \left[\left(\frac{n_1 h}{\rho}\right)^2 + \left(\frac{n_2 g}{\sigma}\right)^2\right](h_{[\rho}g_{\sigma]})^2,
\end{aligned}
\tag{37}
$$

where we have used the notation $h_\rho = \frac{\partial h}{\partial \rho}$, $h_\sigma = \frac{\partial h}{\partial \sigma}$, and $g_{[\rho}g_{\sigma]} = (h_\rho g_\sigma - g_\rho h_\sigma)$ as in (30).

In terms of the coordinates $\rho = R\sin\theta, \sigma = R\cos\theta$ defined by (22), the spherically symmetric limit (30) of (37) follows immediately from by the replacements

$$
h(\rho,\sigma) = Q(R)\sin\theta, \qquad g(\rho,\sigma) = Q(R)\cos\theta,
$$

and using

$$
\partial_\rho = \sin\theta\partial_R + \frac{\cos\theta}{R}\partial_\theta, \qquad \partial_\sigma = \cos\theta\partial_R - \frac{\sin\theta}{R}\partial_\theta.
$$

This limit will be exploited in the numerical constructions.

*Bi-azimuthal symmetry in $D = 5$.* Here, the residual system being three dimensional, we only state the Ansatz

$$
\phi^A = \eta h(r,s,t)n_1^A, \qquad n_1^A = (\cos n_1\varphi_1, \sin n_1\varphi_1), \tag{38}
$$

$$
\phi^{A'} = \eta g(r,s,t)n_2^{A'}, \qquad n_2^{A'} = (\cos n_2\varphi_2, \sin n_2\varphi_2), \tag{39}
$$

$$
\phi^5 = \eta f(r,s,t) \tag{40}
$$

in the notation of (23) and (24).

### *3.6. Tri-azimuthal symmetry*

As noted at the start of this section, we shall simply state the Ansatz here, for six dimensions only, without imposing the symmetry on the energy density building blocks (3). Then in the next section we will use this to calculate the topological charge of the putative solutions in six dimensions, which are not constructed numerically here. The tri-azimuthally symmetric Ansatz for $\phi^a = (\phi^{A_1}, \phi^{A_2}, \phi^{A_3})$, $A_1 = 1, 2$, $A_2 = 3, 4$, $A_3 = 5, 6$:

$$
\begin{aligned}
\phi^{A_1} &= h(\rho,\sigma,\tau)n_1^{A_1}, & n_1^{A_1} &= (\cos n_1\varphi_1, \sin n_1\varphi_1) \\
\phi^{A_2} &= g(\rho,\sigma,\tau)n_2^{A_2}, & n_2^{A_2} &= (\cos n_2\varphi_2, \sin n_2\varphi_2) \\
\phi^{A_3} &= f(\rho,\sigma,\tau)n_2^{A_3}, & n_3^{A_3} &= (\cos n_3\varphi_3, \sin n_3\varphi_3)
\end{aligned}
\tag{41}
$$

where $n_1, n_2$ and $n_3$ are the respective vorticities in the three planes $(x_1, x_2)$, $(x_3, x_4)$ and $(x_5, x_6)$.

## 4. Topological charges and boundary values

In this section, we present in detail the topological charges resulting from the various types of boundary values of the scalar field. This is relevant when subjecting the fields to axial, azimuthal, intermediate bi-azimuthal and tri-azimuthal symmetries in turn. Under each

(symmetry) heading, we will calculate the topological charges in all dimensions $D$ for which the residual subsystem is at most *three* dimensional. This will cover the generic cases, all further examples being superfluous. Subject to axial symmetry, we consider the cases $D=3,4,5,6$. Subject to azimuthal symmetry, we cover only $D=4$. Subject to intermediate symmetry, we take the cases $D=5,6$. For configurations with bi-azimuthal symmetry, we cover $D=4,5$. Subject to tri-azimuthal symmetry, we cover the only possible case $D=6$.

As explained at the end of section 2, it is sufficient to calculate the winding numbers since the topological charges are simply numerical multiples of the latter, which can readily be read off (11). Up to angular volume normalizations $N_D$, these are the surface integrals of the currents (10), hence what we need to calculate are the asymptotic values of the quantities $\hat{x}_\mu \omega_\mu^{(D)}$ to enable us to evaluate the surface integrals

$$I_D = \int \hat{x}_\mu \omega_\mu^{(D)}\Big|_{R=\infty} R^{D-1}\,\mathrm{d}\Omega(\theta_{D-2},\theta_{D-3},\ldots,\theta_1,\varphi), \tag{42}$$

with $\hat{x}_\mu$ being the unit vector, and $\mathrm{d}\Omega(\theta_{D-2},\theta_{D-3},\ldots,\theta_1,\varphi)$ the angular volume element, in $\mathbb{R}^D$.

Here, we will evaluate the angular integrals (42) (a) subject to axial symmetry for $D=3,4,5,6$, (b) subject to azimuthal symmetry for $D=4$ and (c) subject to bi-azimuthal symmetry for $D=4$.

### *4.1. Axial symmetry*

In the case of axially symmetric fields, we will impose the following asymptotic boundary values on the functions $H(r,x_D)$ and $G(r,x_D)$ defined in (28) for $D\geqslant 4$ and in (29) for $D=3$:

$$\begin{aligned} &\lim_{R\to\infty} H(r,x_D) = \sin m\theta_1 \\ &\lim_{R\to\infty} G(r,x_D) = \cos m\theta_1, \qquad\qquad m=1,2,3,\ldots. \end{aligned} \tag{43}$$

The topological charges $q_D$ of the axially symmetric models in $D=3,4,5$ are defined by the integrals (42), divided by the angular volumes $\Omega_{D-1}=2\pi, 2\pi^2, \frac{8\pi^2}{3}$ in each of these dimensions, respectively, by the (volume) integrals

$$q_D = \frac{I_D}{\Omega_{D-1}} = D!\int H^{D-2}(G_R H_{\theta_1} - H_R G_{\theta_1})\,\mathrm{d}R\,\mathrm{d}\theta_1.$$

The surface integrals (42) can be evaluated analytically. In the axially symmetric cases at hand, where the corresponding volume integrals are two dimensional, these become contour integrals in the positive half plane $r[0,\infty), x_D(-\infty,+\infty)$ by virtue of Stokes' theorem. Now the line integral along the $x_D$-axis does not contribute since analyticity requires that $H(\theta_1=0)=H(\theta_1=\pi)=0$, so the only contribution comes from the infinite semicircle, thus reducing (42) to the following one-dimensional angular integrals:

$$I_D^{\text{axial}} = D!\Omega_D \int H^{D-2}(GH_{\theta_1} - HG_{\theta_1})\big|_{R=\infty}\,\mathrm{d}\theta_1, \tag{44}$$

with the exception of the $D=3$ case where axial symmetry coincides with azimuthal symmetry, when

$$I_3 = 2!2\pi n \int H(GH_\theta - HG_\theta)|_{R=\infty}\,\mathrm{d}\theta. \tag{45}$$

Subject to the axially symmetric boundary values (43), the integrals (45) and (44) for $D=3$ and $D=4,5,6$ are evaluated as

$$I_3^{\rm ax} = 4\eta^3\pi n[1-(-1)^m] \tag{46}$$

$$I_4^{\rm ax} = 12\eta^4\pi^2 m \tag{47}$$

$$I_5^{\rm ax} = 32\eta^5\pi^2[1-(-1)^m] \tag{48}$$

$$I_6^{\rm ax} = 5!\eta^6\pi^3 m. \tag{49}$$

We now see from (46) and (48) that in odd $D$ dimensions axially symmetric fields are capable of supporting *zero topological charge* solutions describing an even number $m$ of soliton–antisoliton energy/charge concentrations, as well as *unit topological charge* solutions describing chains [9] for an odd number $m$. As we shall see from the numerical work in section 5.2, these concentrations are located slightly off the $x_D$-axis, forming rings analogous to the nodes on the symmetry axis[5] found in the three-dimensional Yang–Mills–Higgs case. We see by contrast from (47) and (49) that in even $D$ dimensions axially symmetric fields are *not* capable of supporting *zero topological charge* solutions. They describe only multisoliton solutions of the topological charges $m$, the concentrations of charge/energy being located on the $x_D$-axis. (These are the analogues of Witten's axially symmetric instantons [17].) Our numerical solutions in the next section will bear out these conclusions.

Having described candidates for *zero topological charge* solutions in odd dimensions, we proceed to explore prescriptions whereby such solutions in even $D$ dimensions can also be constructed. This is possible only if less stringent symmetry than axial symmetry is imposed on the system, and below we describe two such distinct prescriptions in $D=4$, employing in turn azimuthal and bi-azimuthal symmetries, and one such prescription in $D=6$ employing tri-azimuthal symmetry.

### *4.2. Azimuthal symmetry*

In the case of azimuthal symmetry in $D=4$, the asymptotic boundary values to be imposed on the functions $h(\rho,z,t)$, $f(\rho,z,t)$ and $g(\rho,z,t)$ defined in (33) are

$$\begin{aligned}
&\lim_{R\to\infty} h(\rho,z,t) = \sin m_1\theta_1 \sin m_2\theta_2\\
&\lim_{R\to\infty} f(\rho,z,t) = \sin m_1\theta_1 \cos m_2\theta_2\\
&\lim_{R\to\infty} g(\rho,z,t) = \cos m_1\theta_1, \qquad m_1, m_2 = 1,2,3,\ldots.
\end{aligned} \tag{50}$$

We note here that the asymptotic axially symmetric boundary values are described by one integer $m$ for $D\geqslant 4$ and two integers $(m,n)$ for $D=3$, while those for the azimuthal boundary values for $D=4$ are given in terms of the triple of integers $(m_1,m_2,n)$.

Substituting azimuthal Ansatz (31) in (42) for $D=4$, and using the analyticity requirement that $h(r,t)$ vanishes on the $t$-axis, this reduces to the two-dimensional angular integral

$$I_4^{\rm az} = 4!n\int h\left[h\left(f_{\theta_2}g_{\theta_1}-f_{\theta_1}g_{\theta_2}\right)+f\left(g_{\theta_2}h_{\theta_1}-h_{\theta_1}h_{\theta_2}\right)+g\left(h_{\theta_2}f_{\theta_1}-g_{\theta_1}f_{\theta_2}\right)\right]{\rm d}\theta_1{\rm d}\theta_2, \tag{51}$$

which can readily be evaluated subject to the boundary conditions (50) to yield

$$I_4^{\rm azim} = 12\eta^4\pi^2 m_1 n[1-(-1)^{m_2}]. \tag{52}$$

This accommodates both multisoliton (for *odd* $m_2$) and zero topological charge (for *even* $m_2$) solutions, labelled by the triple of integers $(m_1,m_2,n)$. Unfortunately, the numerical solution of the corresponding field equations involves three-dimensional integration, the task which is beyond the scope of the present work.

[5] Subsequent to the construction of zero charge monopole–antimonopole pairs [7, 8], such charge chains of monopoles and antimonopoles of *unit* topological charge were constructed in [9].

### *4.3. Intermediate symmetries*

In both the $D=5$ and $D=6$ cases discussed in section 3.4, the asymptotic behaviours consistent with finite energy are both stated formally as

$$\begin{aligned}&\lim_{R\to\infty} h(r,s,t) = \sin m_1\theta_1 \sin m_2\theta_2\\ &\lim_{R\to\infty} g(r,s,t) = \sin m_1\theta_1 \cos m_2\theta_2\\ &\lim_{R\to\infty} f(r,s,t) = \cos m_1\theta_1, \qquad m_1, m_2 = 1,2,3,\ldots\end{aligned} \tag{53}$$

augmented by the analyticity condition $h(r=0)=0$, which is crucial in the evaluation of the surface integrals. In both the $D=5$ and $D=6$ cases here, these follow from three-dimensional volume integrals which are formally identical. Up to numerical factors, these are expressed as

$$\begin{aligned}I_{5,6}^{\text{inter}} &\sim \eta^{5,6}(\pi)^{2,3} m_1 m_2 \int \varepsilon_{\mu\nu\rho}\varepsilon^{ABC}\partial_\mu \Xi^A \partial_\nu \Xi^B \partial_\rho \Xi^C \,\mathrm{d}r\,\mathrm{d}s\,\mathrm{d}t\\ &= \eta^{5,6}(\pi)^{2,3} m_1 m_2 \int \varepsilon_{\mu\nu\rho}\varepsilon^{ABC}\,\Xi^A \partial_\nu \Xi^B \partial_\rho \Xi^C \,\mathrm{d}S_\mu,\end{aligned} \tag{54}$$

where we have used the notation $x_\mu = (r,s,t)$, and the triplet function $\Xi^A$, $A=1,2,3$, in the two cases is defined in terms of the functions $(h,g,f)$ as

$$\Xi^A = ((h)^3, g, f) \qquad \text{and} \qquad \Xi^A = ((h)^4, g, f),$$

respectively. The nonvanishing contributions to the surface integral(s) (54) come from the upper hemisphere.

The values of the respective surface integrals in $D=5,6$ are calculated to be

$$I_5^{\text{inter}} = \frac{5\cdot 2^6}{3^2}\eta^5\pi^2 m_2[1-(-1)^{m_1}] \tag{55}$$

$$I_6^{\text{inter}} = 15\eta^6\pi^3 m_1[1-(-1)^{m_2}]. \tag{56}$$

Note the roles of $m_1$ and $m_2$ interchanging in (55) and (56), following from cancellations occurring when evaluating (54).

One sees again that by relaxing axial symmetry and imposing a weaker symmetry, it is possible to support both *multisolitons* of arbitrary topological charges, and *soliton–antisolitons* chains, with *zero* and *nonzero* topological charges in *all dimensions*. Unfortunately, the simplest such examples result in three-dimensional boundary-value problems, which is at present technically too hard a task to perform. The situation is the same in the azimuthal case in $D=4$ above.

### *4.4. Bi-azimuthal symmetry*

Bi-azimuthal symmetry will be applied in $D=4$ and $D=5$, each resulting in a two- and a three-dimensional subsystem, respectively.

$D=4=2+2$. In this case, the fields are described by the bi-azimuthal Ansatz (36). The asymptotic behaviours of the functions $h$ and $g$ in (36) are taken to be

$$\lim_{R\to\infty} h = \sin m\psi, \quad \lim_{R\to\infty} g = \cos m\psi. \tag{57}$$

The topological charge in this case is

$$\begin{aligned}I_4^{\text{bi-azim}} &= \eta^4 3!(2\pi)^2 n_1 n_2 \int \varepsilon_{\mu\nu}\varepsilon^{AB}\partial_\mu \Xi^A \partial_\nu \Xi^B \,\mathrm{d}\rho\,\mathrm{d}\sigma\\ &= \eta^4 3!(2\pi)^2 n_1 n_2 \int (\varepsilon^{AB}\,\Xi^A \partial_\mu \Xi^B)\,\mathrm{d}s_\mu\end{aligned} \tag{58}$$

where we have used the notation $x_\mu = (\rho,\sigma)$ and $\Xi^A = ((h)^2, (g)^2)$.

Using the analyticity conditions $h(\psi = 0) = 0$ and $g\left(\psi = \frac{\pi}{2}\right) = 0$ leads to the vanishing of the line integrals on the $\rho$- and $\sigma$-axes, the nonvanishing contribution coming from the infinite quarter circle contour readily evaluated to yield

$$I_4^{\text{bi-azim}} = \eta^4 2\pi^2 n_1 n_2 [1 - (-1)^m], \tag{59}$$

which supports both multisolitons and zero charge soliton–antisolitons.

$D = 5 = 2 + 2 + 1$. In this case, the fields are described by the bi-azimuthal Ansatz (39). The asymptotic behaviours of the functions $h$, $g$ and $f$ in (39) are taken to be

$$\lim_{R\to\infty} h = \sin m_1\theta \sin m_2\psi, \qquad \lim_{R\to\infty} g = \sin m_1\theta \cos m_2\psi, \qquad \lim_{R\to\infty} f = \cos m_1\theta. \tag{60}$$

The topological charge now reduces to a three-dimensional integral in the residual coordinates $x_\mu = (r, s, t)$

$$\begin{aligned} I_5^{\text{bi-azim}} &= \eta^5 5(2\pi)^2 n_1 n_2 \int \varepsilon_{\mu\nu\rho}\varepsilon^{ABC}\partial_\mu \Xi^A \partial_\nu \Xi^B \partial_\rho \Xi^C \,\mathrm{d}r\,\mathrm{d}s\,\mathrm{d}t \\ &= \eta^5 5(2\pi)^2 n_1 n_2 \int \varepsilon_{\mu\nu\rho}\varepsilon^{ABC}\Xi^A \partial_\nu \Xi^B \partial_\rho \Xi^C \,\mathrm{d}S_\mu, \end{aligned} \tag{61}$$

in which the triplet function $\Xi^A$, $A = 1, 2, 3$, is defined as

$$\Xi^A = ((h)^2, (g)^2, f).$$

The surface integral (61) is then performed to yield

$$I_5^{\text{bi-azim}} = \eta^5 4! n_1 n_2 [1 - (-1)^{m_1}], \tag{62}$$

describing both multisolitons and soliton–antisolitons. Note that only $m_1$, and not $m_2$, features in (62), due to a cancellation in evaluating (61).

### *4.5. Tri-azimuthal symmetry*

This pertains to $D = 6$ only. The asymptotic behaviours of the functions $h$, $g$ and $f$ in the Ansatz (41) are taken to be

$$\begin{aligned} &\lim_{R\to\infty} h = \sin m_1\psi_1 \sin m_2\psi_2 \\ &\lim_{R\to\infty} g = \sin m_1\psi_1 \cos m_2\psi_2 \\ &\lim_{R\to\infty} f = \cos m_1\psi_1. \end{aligned} \tag{63}$$

The topological charge integral in this case is

$$\begin{aligned} I_6^{\text{tri-azim}} &= \eta^6 90(2\pi)^3 n_1 n_2 n_3 \int \varepsilon_{\mu\nu\rho}\varepsilon^{ABC}\partial_\mu \Xi^A \partial_\nu \Xi^B \partial_\rho \Xi^C \,\mathrm{d}\rho\,\mathrm{d}\sigma\,\mathrm{d}\tau \\ &= \eta^6 90(2\pi)^3 n_1 n_2 n_3 \int \varepsilon_{\mu\nu\rho}\varepsilon^{ABC}\Xi^A \partial_\nu \Xi^B \partial_\rho \Xi^C \,\mathrm{d}S_\mu, \end{aligned} \tag{64}$$

where we have used the notation $x_\mu = (\rho, \sigma, \tau)$ and $\Xi^A = ((h)^2, (g)^2, (f)^2)$.

To evaluate the surface integral (64) we need analytic information which comes from finite energy conditions. While we are not displaying here the energy density functional in terms of the functions $(h, g, f)$, it is nonetheless easy to deduce that $h(\psi_1 = 0, \psi_2 = 0) = 0$. $g\left(\psi_1 = 0, \psi_2 = \frac{\pi}{2}\right) = 0$ and $f\left(\psi_1 = \frac{\pi}{2}\right) = 0$. These, together with continuity conditions, imply that the flux (64) out of the three quarter planes $(\rho, \sigma)$, $(\sigma, \tau)$ and $(\tau, \rho)$ vanishes, and hence the only contribution comes from the surface bounding the octant of the 2-sphere with radius $R = \sqrt{\rho^2 + \sigma^2 + \tau^2}$.

Applying the boundary functions (63) on the asymptotic octant the flux (64) yields

$$I_6^{\text{tri-azim}} = \frac{5!\pi^3}{2} n_1 n_2 n_3 \left(\frac{1}{2}[1-(-1)^{m_1}]\right)^4 \left(\frac{1}{2}[1-(-1)^{m_2}]\right)^2, \tag{65}$$

analogous to (59), like which the topological charge vanishes when either $m_1$ or $m_2$ is *even*, and otherwise it is given by the product of the vortex numbers pertaining to each of the azimuthal symmetries imposed.

## 5. Numerical constructions

In this section, we give numerical evidence for the existence of spherically symmetric and axially symmetric solutions in $D=4,5$. In addition, we have constructed solutions with bi-azimuthal symmetry in $D=4$. The solutions of the corresponding $D=3$ model were presented in [11] to which we refer for the latter.

Of course, the most interesting solutions from the viewpoint of understanding zero topological charge are the axially symmetric ones, but the spherically symmetric ones are also presented mainly because the equations of motion in that case allow a thorough asymptotic analysis underpinning the numerical work. Also the spherically symmetric solutions present useful starting profiles for the $D=4$ bi-azimuthally symmetric multisolitons.

Technically, we have restricted ourselves to two-dimensional numerical integration, solutions with azimuthal symmetry in $D \geqslant 4$ representing a difficult numerical challenge which we leave for future work. Also, one should note that only one of the coupling constants $\lambda_i$ is relevant here. For example, one may factor out $\lambda_1$ and, by using a suitable rescaling, one may set $\lambda_2 = 1$, or $\lambda_3 = 1$, without any loss of generality.

To simplify the picture, in this section we shall note $\theta_{D-2} = \theta$ and $x_D = z$. Also, for all configurations, the total mass/energy $M$ (which equals the total action) is computed by integrating the corresponding reduced energy functionals.

### *5.1. Spherically symmetric solutions*

Considering the Ansatz (26), the reduced one-dimensional weighted energy density reads

$$\begin{aligned} E = R^{D-1}\mathcal{E} = R^{D-1}\Bigg(&\lambda_1(Q^2-1)^4\left(Q'^2+(D-1)\frac{Q^2}{R^2}\right)+2(D-2)\lambda_2(Q^2-1)^2\frac{Q^2}{R^2} \\ &\times\left(2Q'^2+(D-2)\frac{Q^2}{R^2}\right)+6\lambda_3(D-1)(D-2)\frac{Q^4}{R^4}\left(3Q'^2+(D-3)\frac{Q^2}{R^2}\right)\Bigg) \end{aligned} \tag{66}$$

which leads to the following differential equation:

$$\begin{aligned} &\left[2R^{D-1}Q'\left(\lambda_1(Q^2-1)^4+4\lambda_2(D-2)(Q^2-1)^2\frac{Q^2}{R^2}+18\lambda_3(D-1)(D-2)\frac{Q^4}{R^4}\right)\right]' \\ &\quad = R^{D-2}(2\lambda_1(Q^2-1)^3(4Q'^2+5(D-1)\frac{Q^2}{R^2}-\frac{(D-1)}{R^2}+4\lambda_2\frac{(D-1)}{R^2}Q(Q^2-1) \\ &\qquad +36\lambda_3\frac{(D-1)(D-2)}{R^4}Q^3\left(2Q'^2+(D-3)\frac{Q^2}{R^2}\right). \end{aligned}$$

The solutions of this equation have been constructed numerically, for a range of the parameters $\lambda_i$. We follow the usual approach and, by using a standard ordinary differential equation solver, we evaluate the initial condition

$$Q(R) = bR - \frac{2b^3\lambda_1}{3(\lambda_1+12b^2(\lambda_2+9b^2\lambda_3))}R^3 + O(R^5), \qquad \text{for} \quad D=4, \tag{67}$$

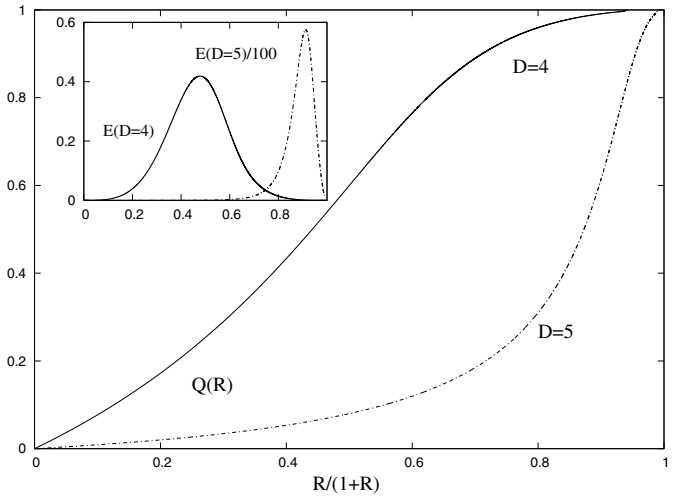


**Figure 1.** The scalar function $Q$ and weighted energy density $E$ of two typical $D = 4$ and $D = 5$ spherically symmetric solutions, with $\lambda_1 = 1$, are shown as a function of the compactified radial coordinate $R/(1 + R)$.

$$Q(R) = bR - \frac{2(b^3\lambda_1 + 4b^5\lambda_2 - 2)}{7(\lambda_1 + 16b^2\lambda_2 + 216b^4\lambda_3)}R^3 + O(R^5), \qquad \text{for} \quad D = 5 \tag{68}$$

at $R = 10^{-6}$ for global tolerance $10^{-14}$, adjusting for the shooting parameter $b$ and integrating towards $R \to \infty$. The behaviour of finite energy solutions for the large values of $R$ is

$$Q(R) = 1 + c\,\mathrm{e}^{-\frac{2}{3}\sqrt{\lambda_2/\lambda_3}R} - \frac{9\lambda_3}{4\lambda_2}\frac{1}{R^2} - \frac{243\lambda_3^2}{16\lambda_2^2}\frac{1}{R^4} + O(1/R^6), \qquad \text{for} \quad D = 4, \tag{69}$$

$$Q(R) = 1 + c\,\mathrm{e}^{-\frac{2}{3}\sqrt{\lambda_2/\lambda_3}R} - \frac{9\lambda_3}{2\lambda_2}\frac{1}{R^2} + \frac{81\lambda_3^2}{2\lambda_2^2}\frac{1}{R^4} + O(1/R^6), \qquad \text{for} \quad D = 5, \tag{70}$$

where $c$ is a free parameter (the corresponding expressions for the $D = 3$ model are given in [11]). For all cases considered, the solutions with the correct asymptotics are found when the first derivative of the scalar function $Q(R)$ evaluated at the origin, $Q'(0) = b$, takes on a certain value, which is a function of $\lambda_i$.

The profiles of typical $D = 4, 5$ solutions are presented in figure 1 for $\lambda_1 = \lambda_2 = \lambda_3 = 1$. The weighted energy density, as given by (66), is also exhibited (one should note the different length scales of the $D = 4$ and $D = 5$ solitons). Similar to the $D = 3$ case, no multinode radial solutions were found, although we have no analytical argument for their absence.

### *5.2. Axially symmetric solutions*

Scalar solitons with axial symmetry are found by taking $m \geqslant 2$ in the boundary conditions at infinity (43). The two-dimensional weighted energy density $E(R, \theta) = R^{D-1}\sin^{D-2}\theta\mathcal{E}(R, \theta)$ and the set of two coupled nonlinear elliptic partial differential equations satisfied by the functions $H(R, \theta)$, $G(R, \theta)$ can easily be derived by using the reduced building blocks (30) and we shall not present them here. These equations are solved numerically, subject to the boundary conditions

$$H|_{R=0} = 0, \qquad \partial_R G|_{R=0} = 0, \tag{71}$$

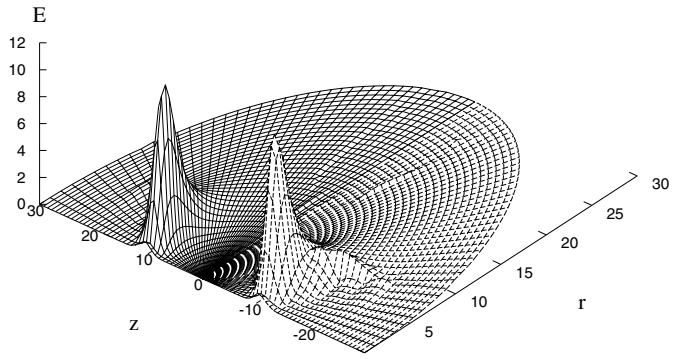


**Figure 2.** A three-dimensional plot of the weighted energy density $E(R,\theta)$ of a $D=5, m=2$ axially symmetric solution with $\lambda_1=\lambda_2=1, \lambda_3=75$.

at the origin and (43) at infinity[6] (we have restricted our analysis to $m=2$ solutions; the $m=1$ case corresponds to spherically symmetric configurations). Considering solutions with parity reflection symmetry, the equations are integrated in the $0\leqslant\theta\leqslant\pi/2$ region. The boundary conditions satisfied at the limits of the $\theta$-interval are

$$H|_{\theta=0}=\partial_\theta G|_{\theta=0}=0,\ \partial_\theta H|_{\theta=\pi/2}=G|_{\theta=\pi/2}=0. \tag{72}$$

The absence of suitable starting profiles makes this problem extremely difficult[7]. The numerical calculations were performed with the software package CADSOL/FIDISOL, based on the Newton–Raphson method [18].

The numerical error for the functions is estimated to be of the order of $10^{-2}$ or lower for most of the axially symmetric configurations.

Solutions with $m=2$ of the corresponding $D=3$ model were discussed in [11]. In that case it was possible to distinguish two individual components (e.g. the modulus of the scalar field $|\phi|=\sqrt{\phi_1^2+\phi_2^2}$ always possesses two distinct zeros on the $z$-axis).

Our $D=4,5$ results indicate that this is a generic feature of all axially symmetric solutions. In figure 2, we present a three-dimensional plot of the weighted energy density (the reduced Lagrangian) $E(R,\theta)$ of a typical $D=5, m=2$ axially symmetric solution as a function of $r$, $z$ (here $\lambda=\lambda_2=1, \lambda_3=75$). The modulus of the scalar field $|\varphi|=\sqrt{H^2+G^2}$ of a $D=4$ solution with $\lambda=\lambda_2=1, \lambda_3=8$ is presented in figure 3. We have found that $|\varphi|$ always possesses two zeros at $\pm d/2$ on the $z$-symmetry axis, the positions of the nodes depending on the value of the coupling constants $\lambda_i$. The total action of these solutions, as given by the integral of $E(R,\theta)$, increases with increasing $\lambda_i$.

Interestingly enough, the weighted energy density $E(R,\theta)$ possesses a saddle point at the origin, the maxima being localized at $z=\pm d/2$, at a nonzero value of $r$, $r=r_0$. This feature, already present in the $D=3$ case (see figure 4 in [11]) is enhanced for the higher dimensional configurations, in contrast with the $D=3$ Yang–Mills–Higgs [8, 9] where the concentrations of energy are located exactly on the symmetry axis.

Although the profiles of the axially symmetric solutions look qualitatively the same for $D=3,4,5$, their physical significance is very different. For $D=4$ they describe two distinct

[6] In the numerical algorithm we have employed a compactified radial coordinate $x=R/(1+R)$, such that spatial infinity corresponds to $x=1$.

[7] We managed to overcome this difficulty by improving, in successive steps, an initial guess solution constructed with suitable trial functions which interpolates between the asymptotics (71), (43).

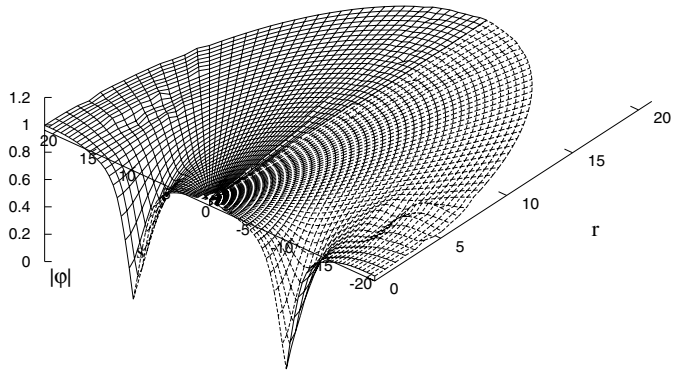


**Figure 3.** The modulus of the scalar field $|\varphi| = \sqrt{H^2 + G^2}$ is shown as a function of the coordinates $r$ and $z$ for a typical $D = 4, m = 2$ axially symmetric solution. Here $r = R \sin\theta$, $z = R \cos\theta$.

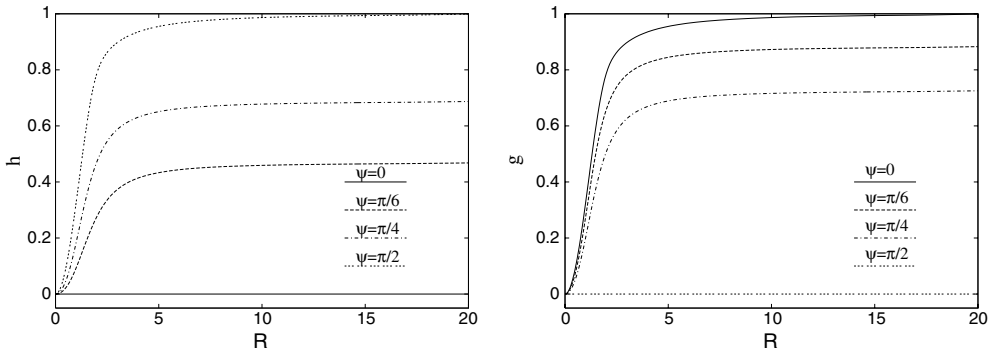


**Figure 4.** The profiles of the scalar functions $h$ and $g$ are shown for a typical $D = 4$ bi-azimuthally symmetric solution with $n_1 = n_2 = 2, \lambda_1 = \lambda_2 = \lambda_3 = 1$.

solitons sitting at $(z = \pm d/2, r = r_0)$, while in three and five dimensions the solutions represent a pair of soliton–antisoliton with zero topological charge.

It would be interesting to construct higher $m$ solutions, describing for an odd dimension soliton–antisoliton chains, in analogy with the situation in YMH theory [9].

### *5.3. Solutions with bi-azimuthal symmetry*

To obtain $D = 4, m = 1$ configurations with bi-azimuthal symmetry, we employ the $n = 1$ spherically symmetric solutions discussed in section 5.1 for starting profiles and increase the values of $n_1, n_2$ slowly. The iterations converge, and repeating the procedure one obtains in this way the solutions for arbitrary $n$. The physical values of $n_1, n_2$ are integers. We have studied solutions with $1 \leqslant n_1, n_2 \leqslant 9$. The weighted energy density $E(R, \psi)$ can be written in terms of the reduced building blocks (37). The two scalar functions $h(R, \psi)$ and $g(R, \psi)$ satisfy the boundary conditions

$$h|_{R=0} = g|_{R=0} = 0 \tag{73}$$

at the origin, (57) at infinity, and

$$h|_{\psi=0} = \partial_\psi g|_{\psi=0} = 0, \qquad \partial_\psi h|_{\psi=\pi/2} = g|_{\psi=\pi/2} = 0 \tag{74}$$

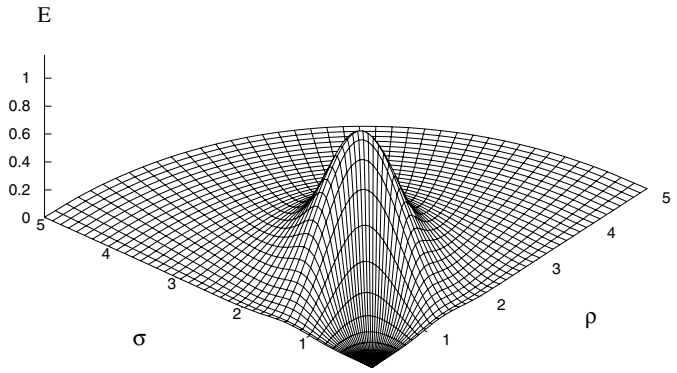


**Figure 5.** A three-dimensional plot of the weighted energy density $E(\rho,\sigma)$ of the $D=4$ bi-azimuthally symmetric solution presented in figure 4.

on the $\rho$- and $\sigma$-axes. The field equations have been solved by using the same methods employed in the axially symmetric case but now with much better accuracy, the typical numerical error being of the order of $10^{-4}$ or smaller.

As expected, the bi-azimuthally symmetric solutions exhibit a very different picture. A general feature of all $m=1$ solutions with $n_1=n_2$ is that the weighted energy density $E(R,\psi)$ possesses one maximum on the $\psi=\pi/4$ axis (corresponding to the $\rho=\sigma$ surface), it being possible to distinguish only one individual concentration of the action. In this respect, the bi-azimuthally symmetric multisolitons of this model are qualitatively similar to those of the models featuring gauge fields, as discussed recently in [10, 19]. In contrast to the latter however, where only solutions with $n_1=n_2$ were found, here we noticed the existence of finite mass solutions with $n_1\neq n_2$. The maximum of the weighted energy density moves inward with increasing $n_1, n_2$.

In figure 4, the profiles scalar functions $h$ and $g$ of the typical bi-azimuthally symmetric solution are shown for several angles as a function of the radial coordinate $R$ (with $\lambda_1=\lambda_2=\lambda_3=1$ in this case). A three-dimensional plot of the weighted energy density of a typical $m=1, n_1=n_2=2$ configuration is presented in figure 5. We have also studied the mass dependence of the bi-azimuthally symmetric solutions on the coupling constants $\lambda_i$. From the numerical results, we observed some features of the solutions, without attempting to give an analytic explanation. The most peculiar of these is the fact that finite mass solutions persist for a small but finite range of negative $\lambda_2\leqslant 0$. No such solutions can be justified by the topological lower bounds.

When $\lambda_1$ or $\lambda_2$ are varied, the maximum of the weighted energy density moves inwards with the increasing value of the respective coupling constant, while the opposite behaviour to this is found when $\lambda_3$ is varied. Yet another property of multisolitons is observed. It turns out that the mass of a solution $M(n_1,n_2)$, whose topological lower bound given by (59) to be $4\pi^2 n_1 n_2$, is quantitatively quite close to $n_1 n_2 M(1,1)$. This means that the deviation of the value of $M(n_1,n_2)$ from its lower bound value is proportionate to the deviation of the value of $M(1,1)$ from its respective lower bound value, implying that composite solitons have rather low binding energies. On the other hand, in all cases studied, it turns out that $M(n_1,n_2) > n_1 n_2 M(1,1)$, albeit by a small amount quantitatively. This in turn suggests that the composite states are unstable against decay into the lowest mass constituents. This property of Goldstone solitons is in direct contrast to the Skyrme soliton (and presumably

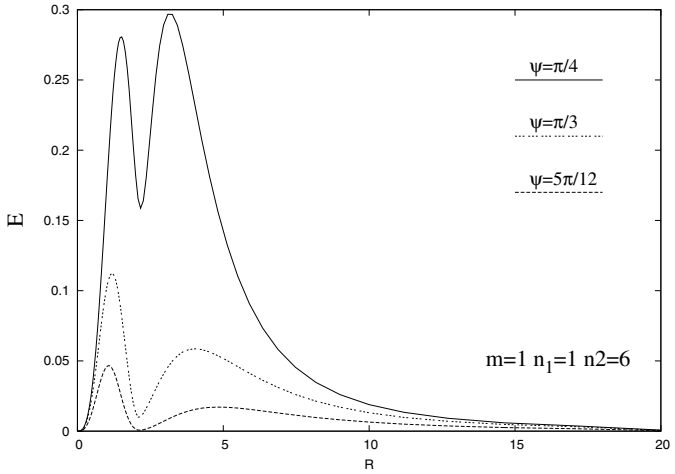


**Figure 6.** The weighted energy density $E$ is shown for a $D = 4$ bi-azimuthally symmetric solution presenting two localized elementary constituents.

solitons of higher dimensional $O(D+1)$ sigma models), making them unsuitable to describe bound states.

Yet another surprising but not counterintuitive property observed is, that while multisolitons of masses $M(n_1, n_2)$ exhibit one single peak of the weighted energy density for *small* values of $|n_1 - n_2|$, when $|n_1 - n_2|$ becomes *large* the weighted energy density develops two separated peaks (see figure 6).

More complicated bi-azimuthal solutions with $m \geqslant 2$ are likely to exist. These configurations would describe composite bound states, rather analogous to the monopole–antimonopole chains of the Yang–Mills–Higgs model [9]. Our preliminary numerical results already indicate the existence of zero topological charge $m = 2$ configurations with bi-azimuthal symmetry in $D = 4$, with $n_1 = n_2 = 2$. We found that there were no $m = 2$ solutions with $n_1 = n_2 = 1$, just as for the pure YM model whose instanton–antiinstanton solutions are constructed in [10]. Again as in [10], the weighted energy density exhibits two distinct maxima on the $\psi = \pi/4$ axis. In the absence of suitable starting profiles, however, the numerical accuracy of these solutions turned out to be much lower in this case[8].

We hope to return to a systematic discussion of these solutions, together with a generalization to higher dimensions.

## 6. Summary and conclusions

The overriding aim of this work is to examine the conditions that enable the construction of zero topological charge solutions in classical field theories, which otherwise support topologically stable (multi-)soliton solutions with nonvanishing topological charge. We have shown that the conditions in question are those of (a) subjecting the system to the requisite symmetry, which in practice is what is done anyway when constructing (multi-)solitons and (b) by

[8] We started the numerical process by employing a guess solution constructed with a suitable trial function that contains several free parameters whose values are then tuned. However, improving the accuracy of these profiles has proven more difficult than in the case of the axially symmetric configurations, where a similar approach has been employed.

requiring special types of the boundary conditions that differ essentially from those employed for (multi-)solitons.

Our symmetry analysis covers dimensions $D = 3, 4, 5, 6$, namely both odd and even examples in $6 \geqslant D \geqslant 3$, while the solutions constructed numerically to underpin our findings are limited to $D \leqslant 5$. The reason for this restriction is that the boundary-value problems in more than two dimensions are beyond the scope of the present work. The case $D = 2$ is irrelevant, being too small to accommodate requirements (a) and (b). The case $D = 3$, while it is the first nontrivial example, is rather special since in that case *axial* and *azimuthal* symmetries coincide. We have chosen to carry out this investigation in the framework of the simplest possible field theoretic model, irrespective of its applicability to physical problems. This is a symmetry breaking Goldstone-type model in $D$ Euclidean dimensions, whose energy density functional depends on a $D$ component scalar field $\phi^a$, $a = 1, 2, \ldots, D$. This choice is motivated by the fact that the topological charges in such models are the simplest available examples, being up to constant multiples of the *winding numbers* of $\phi^a$ in $\mathbb{R}^D$. It should be emphasized however that our conclusions hold in the other classical field theories that support solitons in these dimensions, namely the sigma models and the non-Abelian gauge field systems (including the Higgs fields).

Our conclusions can be summarized as follows:

- The field $\phi^a$ asymptotically tends to a unit vector $\hat{\phi}^a$, which depends exclusively on angular variables, the radial variable being infinite. Precisely what these angular variables depend on the symmetry imposed. To analyse qualitatively distinct possibilities, we have found it sufficient to impose symmetries that result in the residual subsystems of no more than *three* dimensions. It is superfluous to consider weaker symmetries resulting in four or higher number of effective degrees of freedom, since these do not result in qualitatively new features as far as the existence of multisolitons and soliton–antisoliton chains is concerned.
- There are two types of symmetries employed. First, spherical (rotational) symmetry in an $N$-dimensional subspace of $\mathbb{R}^D$. For $N = D - 1$, this is *axial* symmetry resulting in *two* effective degrees of freedom. At the other extreme, $N = 2$, this is *azimuthal* symmetry resulting in an effective $(D-2)$-dimensional subsystem. Accordingly, we have restricted to $D = 3, 4$ in the case of *azimuthal* symmetry. Intermediate values of $N$ subject to this restriction are $N = 3$ in $D = 5$ and $N = 4$ in $D = 6$. We have described these as *intermediate* symmetries. Second, we impose *multi-azimuthal* symmetries, composed of azimuthal symmetries in pairs of coordinates. Again, subject to limiting our considerations to three effective degrees of freedom, these are *bi-azimuthal* symmetry in $D = 4, 5$ and *tri-azimuthal* symmetry in $D = 6$. The residual system after symmetry imposition depends on the radial coordinate and the remaining angular coordinates, and the number of unknown functions is the same as the dimensionality of the residual subsystem. In all cases, the azimuthal angles are all integrated out and the remaining angular dependence is on *polar* angles $\{\theta_i\}$ $(0 \leqslant \theta \leqslant \pi)$ and *semi-polar* angles $\{\psi_I\}$ $\left(0 \leqslant \psi_I \leqslant \frac{\pi}{2}\right)$, $i$ and $I$ labelling the residual polar and semi-polar angles, respectively.
- The asymptotic field $\hat{\phi}^a$ is parametrized by the residual angular variables $\{\theta_i\}$ and $\{\psi_I\}$ only. The other angular variables, that include *all azimuthal* angles, are integrated out. Consistently with the requirements of finite energy and analyticity, the most general as $\hat{\phi}^a$ is encoded by $\{\theta_i\}$ and $\{\psi_I\}$ is via

$$\{m_i\theta_i\}, \qquad \{m_I\psi_I\}, \qquad m_i, m_I \quad \text{integers.} \tag{75}$$

It is important to stress that the integers $(m_i, m_I)$ in (75) appear *only* in the asymptotic field $\hat{\phi}^a$, and that they *do not* parametrize the field $\phi^a$ everywhere. Throughout this text, we have reserved the letter $m$ to these $m$-numbers. In contrast we label the *vorticity* associated with each azimuthal symmetry, on which the field $\phi^a$ everywhere depends, by the letters $\{n\}$. Thus, the $n$-numbers which count the winding in each azimuthal plane are on a completely distinct footing as opposed to the $m$-numbers which serve only to select the boundary values imposed. All solutions with $m = 1$ describe topologically stable[9] multisolitons whose topological charges are encoded with the $n$-numbers, $\{n\}$. The topological charges of soliton–antisoliton chains with even $m$ are *zero*, while those of odd $m$ are *nonzero*, and depend on $\{n\}$. In the special case of axial symmetry in $D \geqslant 4$, when no $n$-number occurs, the topological charges in even $D$ are labelled by an $m$-number.

The numerical constructions in section 5 underpin the above conclusions. Both (multi-)solitons and soliton–antisoliton solutions have been constructed like for the $D = 3$ case in [11], whose results are extended to higher dimensions in the present work. Various features found there are shared by higher dimensional axially symmetric solutions. In particular, the profiles of the scalar functions have rather similar shapes. The numerical constructions in the present work are limited to two-dimensional boundary-value problem involving two functions, so that we only present axially symmetric solutions in $D = 4, 5$ (and $D = 3$ in [11]) and bi-azimuthally symmetric solutions in $D = 4$.

The axially symmetric solutions constructed in both [11] and in section 5.2 are limited in their scope to solutions with asymptotic behaviour characterized by $m$-number equal to 1 and 2. In the $D = 3$ case [11], these are multisolitons with $m = 1$ and higher $n$-numbers, and to soliton–antisoliton pairs with $m = 2$ and $n$-number equal to 1. In $D = 3$, like for the YMH monopoles (see, e.g., [20, 21]), the energy density of the multisolitons is concentrated at the origin, and when $m = 2$ there occur two concentrations distributed symmetrically on the 3-axis. While we expect that solitons with $m \geqslant 2$ and with $n = 1$ would describe chains of solitons and antisolitons on the 3-axis, and when $n \geqslant 3$ rings would form, like for the monopoles in the YMH model observed in [9], this has not been carried out in [11]. Here, axially symmetric solutions in $D = 4, 5$ are constructed in section 5.2. The $m = 2$ solutions in $D = 5$ are similar to the $m = 2, n = 1$ soliton–antisoliton solutions in $D = 3$, i.e. they describe two distinct peaks of the weighted energy density on the 5-axis of equal and opposite charges. But there is no $n$-number in $D = 5$ so here the analogy with $D = 3$ stops. The $m = 2$ axially symmetric solutions in $D = 4$ also describe two distinct particles located on the 4-axis, but unlike those of $D = 3, 5$ both the peaks of the energy density have the same topological charge. These are multisolitons, qualitatively similar to the axially symmetric Witten multiinstantons [17]. This illustrates that for axially symmetric fields with $m$-number higher than 1 the peaks of the weighted energy density are situated on the (symmetry) $D$-axis, such that in odd dimensions their charges have alternating signs, while in even dimensions all the charges have the same sign.

There is one final property of axially symmetric solutions worth remarking on. In gauge field systems, namely the $D = 3$ YMH configurations as our only example, the zero charge $m = 2$ solutions have a positive binding energy with respect to decay into two charge-1 monopoles [8]. By contrast, the multisolitons and the soliton–antisoliton solutions of the Goldstone models have negative binding energies. Because the data available to us are

[9] These solutions are not *absolutely* stable since no Bogomol'nyi-type bounds are saturated in these models. Rather, the stability in question is a consequence of the energy respecting topological lower bound, like in the case of Skyrmions [20]

not sharp enough, we have not displayed this quantitatively either with a plot or a table in section 5.2. Nevertheless, the observed qualitative trend is unmistakable.

The bi-azimuthally symmetric solutions in $D=4$ constructed in section 5.3 have their analogue in the bi-azimuthal YM instantons given in [10]. Like in that case there is an $n$-number associated with each (of the two) azimuthal symmetries, $n_1$ and $n_2$, and the topological charge is proportional to $n_1 n_2$ (see (62)). Unlike in [10] however, where finite action solutions occur only for one integer $n_1 = n_2 = n$, here there are solutions for distinct $n_1 \neq n_2$. For $m$-number equal to 1 with $n_1 = n_2 = n$ the action density has only one peak which like in the YM example [10] is not situated at the origin. Rather, it peaks at a numerically determined distance from the origin on the $\psi = \frac{\pi}{4}$ axis, with $\psi$ being the unique semi-polar angle. The situation is different in the $(m=1)$ $n_1 \neq n_2$ case. There the action density breaks up into two distinct peaks on the $\psi = \frac{\pi}{4}$ axis, and the centres of these peaks move away from each other as $|n_1 - n_2|$ increases. Another point of contrast with the YM case, where the multiinstantons do form bound states, the corresponding multisolitons here do not form bound states. For all configurations we have studied, the energy of the $n_1, n_2$ multisolitons of our model is greater than that of $n_1 n_2$1-solitons. Moreover, it turns out that this deficit of binding energy increases with increasing $n_1, n_2$. We have also verified that $m=2$ solutions carrying zero topological charge (see (62)) exist, in the $n_1 = n_2 = 2$ case, but have not supplied quantitative data here. These present two distinct peaks of the weighted energy density like in the YM case [10]. Our numerical results here were not sufficiently accurate to enable us to estimate whether the binding energy preventing the decay of this solution into two charge-2 $(m=1)$ multisolitons is positive or negative. Likewise for the same reason, we did not increase $n_1$ and $n_2$ to values higher than 3, to see what the analogues of the rings forming in the $D=3$ YM example [8] are. (Such ring-like configurations were discovered recently in the bi-azimuthal gauge field configurations with $n=3$ in [19], implying their occurrence here.)

This completes the summary of our results. We now make some final, general comments. We have seen that most of the geometrical and topological properties of the multisoliton and soliton–antisoliton solutions in the Goldstone models studied here are broadly similar both to the YMH example [8, 9] in $D=3$ and the YM example [10] in $D=4$. There are however some notable differences, first that the binding energies of our multisolitons are negative as opposed to those of their gauge field counterparts [8–10], which are positive. Then there is the difference between the $D=4$ bi-azimuthal Goldstone solitons, where the two vorticities ($n$-numbers) can be different, and the $D=4$ YM instantons for which the two vorticities must be equal. More recently, the $SU(2)$ YM-dilaton system in $4+1$ dimensions was analysed and the static bi-azimuthally symmetric solutions were studied in [19]. There too the numerical results indicated that the two $n$-numbers had to be equal $n_1 = n_2$. It appears therefore that this restriction $(n_1 = n_2)$ applies to bi-azimuthally symmetric gauge fields, but not to the Goldstone fields. It is likely this feature may persist in multi-azimuthal systems too, but since this conclusion is reached only on the basis of numerics it is beyond the scope of the present work.

Based on what we have learnt about the general similarities in the different models supporting topologically nontrivial lumps studied here and in [8, 9, 10, 19], we would speculate that similar analogous properties can be expected for the lump solutions in various sigma models, e.g. $O(D+1)$ models on $\mathbb{R}^D$, or the corresponding Grassmannian sigma models on $\mathbb{R}^{2N}$ or indeed their gauged counterparts. One aspect in which it would have been more appropriate to use the $O(D+1)$ models on $\mathbb{R}^D$ instead of the Goldstone models, featuring negative binding energies, is that the $O(D+1)$ models would be expected to feature positive binding energies, based on our knowledge of the $O(3+1)$ model on $\mathbb{R}^3$, namely the celebrated Skyrme model. Certainly, the simple analysis of the topological charges and

boundary conditions given in section 4 can be extended systematically and without obstacles to the sigma model counterparts of the scalar Goldstone fields. This was eschewed because the numerical constructions for the sigma models, in particular the practical task of imposing the boundary conditions, are very much harder. On the physical level, we have found that the higher mass Goldstone solitons are unstable against decay into their lowest mass constituents, in contrast to the Skyrme solitons.

One last comment concerns a common feature of zero topological charge bi-azimuthal solutions to both gauge field systems, namely those studied in [10, 19] and to the corresponding Goldstone model studied here. These are both solutions with $m$-number equal to 2. In the former case, the numerical results indicated that the simplest such a solution was that with $n$-number equal to 2 and not $n = 1$. Likewise in the case at hand, it turned out that there existed no solution for $n_1 = n_2 = 1$, the simplest solution being characterized by $n_1 = 1, n_2 = 2$. It is interesting that this observation is consistent with the results of the numerical analysis of Krusch and Sutcliffe [22] in the context of the zero baryon charge solutions of the Skyrme model. The analytic analysis of Sadun and Segert [3] is also very interesting, which proves the existence of non-self-dual instantons (e.g. the $m = 3$ instantons in [10]), their proof excludes topological charge-1 instantons (e.g. our $m = 3$ instantons with $n = 1$ whose topological charge is equal to $n^2 = 1$). This is a rather subtle but pervasive feature, which we cannot analyse further here.

## Acknowledgment

This work was carried out in the framework of Science Foundation Ireland (SFI) Research Frontiers Programme (RFP) project RFP07/FPHY330.

## References

[1] Belavin A A, Polyakov A M, Shvarts A S and Tyupkin Yu S 1975 *Phys. Lett.* B **59** 85
[2] Sibner L M, Sibner R J and Uhlenbeck K 1989 *Proc. Natl Acad. Sci. USA* **86** 860
[3] Sadun L and Segert J 1992 *Commun. Math. Phys.* **145** 363
[4] Bor G 1992 *Commun. Math. Phys.* **145** 393
[5] Taubes C H 1982 *Commun. Math. Phys.* **86** 257
[6] 't Hooft G 1974 *Nucl. Phys.* B **79** 276
Polyakov A M 1974 *Pisma Zh. Eksp. Teor. Fiz.* **20** 430
Polyakov A M 1974 *JETP Lett.* **20** 194 (Engl. Transl.)
[7] Rüber B 1985 Eine axialsymmetrische magnetische Dipollösung der Yang–Mills–Higgs–Gleichungen *Thesis* University of Bonn
[8] Kleihaus B and Kunz J 2000 *Phys. Rev.* D **61** 025003
[9] Kleihaus B, Kunz J and Shnir Y 2004 *Phys. Rev.* D **70** 065010 (*Preprint* hep-th/0405169)
[10] Radu E and Tchrakian D H 2006 *Phys. Lett.* B **636** 201 (*Preprint* hep-th/0603071)
[11] Paturyan V, Radu E and Tchrakian D H 2006 *J. Phys. A: Math. Gen.* **39** 3817 (*Preprint* hep-th/0509056)
[12] Ioannidou T A and Sutcliffe P M 1999 *Phys. Lett.* B **467** 54 (*Preprint* hep-th/9907157)
[13] Tchrakian D H 1985 *Phys. Lett.* B **150** 360
Tchrakian D H 1993 Yang–Mills hierarchy *Differential Geometric Methods in Theoretical Physics Int. J. Mod. Phys. (Proc. Suppl.) A* vol 3 ed C N Yang, M L Ge and X W Zhou p 584
[14] Kleihaus B, O'Keeffe D and Tchrakian D H 1998 *Phys. Lett.* B **427** 327 (see for example the model in $D = 3$)
O'Brien G M and Tchrakian D H 1989 *Mod. Phys. Lett.* A **4** 1389 (and see for example the model in $D = 4$)
[15] Tchrakian D H 1991 *J. Phys. A: Math. Gen.* **24** 1959
Tchrakian D H 1990 *Phys. Lett.* B **244** 458
[16] Nahm W and Tchrakian D H 2004 *J. High Energy Phys.* JHEP04(2004)075
[17] Witten E 1977 *Phys. Rev. Lett.* **38** 121

[18] Schönauer W and Weiß R 1989 *J. Comput. Appl. Math.* **27** 279
Schauder M, Weiß R and Schönauer W 1992 *The CADSOL Program Package* Interner Bericht No 46/92 (Universität Karlsruhe)
[19] Radu E, Shnir Y and Tchrakian D H 2007 *Phys. Rev.* D **75** 045003 (*Preprint* hep-th/0611270)
[20] Manton N S and Sutcliffe P 2004 *Topological Solitons* (Cambridge: Cambridge University Press)
[21] Shnir Y M 2005 *Magnetic Monopoles* (Berlin: Springer)
[22] Krusch S and Sutcliffe P 2004 *J. Phys. A: Math. Gen.* **37** 9037 (*Preprint* hep-th/0407002)